# Atmospheric S and lithospheric Pb in sulphides from the 2.06 Ga Phalaborwa phoscorite-carbonatite Complex, South Africa

Robert Bolhar [a*], Martin J. Whitehouse [b], Lorenzo Milani [c], Nivea Magalhães [d], Suzanne D. Golding [e], Grant Bybee [a], Loic LeBras [a], Andrey Bekker [f]

[a] School of Geosciences, University of the Witwatersrand, Johannesburg 2001, South Africa

[b] Swedish Museum of Natural History, Stockholm SE104 05, Sweden

[c] Department of Geology, University of Pretoria, Pretoria 0002, South Africa

[d] Department of Geology, University of Maryland, College Park, MD 20742, USA

[e] School of Earth & Environmental Sciences, University of Queensland, Brisbane 4072, Australia

[f] Department of Earth and Planetary Sciences, University of California, Riverside, CA 92521, USA

**Highlights**

• Pb isotopes indicate sulphide mineralization age and contribution of evolved (crustal) material.

• MIF-S require recycling of pre 2.43 Ga atmospheric sulphur into carbonatite-phoscorite melts.

• Mantle plume melts assimilated subduction-metasomatized subcontinental lithospheric mantle.

*Keywords:* Great Oxidation Event, sulphur isotopes, lead isotopes, Phalaborwa Complex, sub-continental lithospheric mantle, magmatic sulphides

## ABSTRACT

Lead and multiple sulfur isotope compositions were measured in-situ by SIMS on sulphide minerals from phoscorites and carbonatites of the ca. 2.06 Ga Phalaborwa Complex in South Africa. Additionally, sulphide mineral separates and bulk-rock samples were analyzed with IRMS methods to confirm SIMS data. Lead isotope

ratios define a trend stretching from unradiogenic to highly radiogenic ratios corresponding to a Pb-Pb regression date of 2054 ± 99 Ma. This apparent date is consistent with the timing of emplacement and thus provides an age estimate for the sulphide mineralization. The least radiogenic Pb isotope compositions overlap, and the regression line intersects, a hypothetical mixing line between MORB mantle and an upper crustal reservoir at ca. 2.1 Ga, suggesting that either a significant quantity of crustal Pb contributed to sulphide mineralization, or that sulphidic xenomelts were derived from an isotopically enriched mantle source. Sulphur isotope ratios of individual sulphide minerals obtained by SIMS are highly variable ($\delta^{34}S$: -15 to +15 ‰ V-CDT) and, importantly, reveal the contribution of pre-Great Oxidation Event (GOE) atmospheric sulfur with mass-independent isotope fractionation ($\Delta^{33}S = \delta^{33}S - [(1+\delta^{34}S)^{0.515}-1]\times1000 \neq 0.0$ ‰). Mass-independent sulphur isotope fractionation is also revealed by sulphur isotope ratios measured on sulphide mineral separates ($\Delta^{33}S$: 0.2 to 0.7 ‰) and bulk-rock samples ($\Delta^{33}S$: 0.2 to 0.4 ‰). Generally, the range of sulphur isotope ratios obtained with SIMS is much larger than that observed in non-SIMS data, possibly reflecting isotopic variability at the μm scale, resolvable only with microbeam measurements. Various sources and mechanisms by which supracrustal material may have been incorporated into mantle-derived carbonatite-phoscorite magmas are assessed, taking into account that geological evidence for the presence of sedimentary material available for assimilation during shallow-level magma emplacement is lacking. Given the variability in S and Pb isotopic compositions, it is inferred that pre-GOE surficial Pb and S were not derived from asthenospheric mantle contaminated with supracrustal materials. Instead, whole-rock trace element compositions, in concert with published geochemical and petrological evidence, are consistent with interaction of asthenospheric, plume-derived melt with

compositionally heterogeneous lithospheric mantle that was metasomatically modified by fluids and melts released from a subducting slab. Despite geochemical and geochronological similarities with the 2055 Ma Busvheld Complex, lead and sulphur isotope data for both complexes are resolvably different, pointing to distinct lithospheric mantle sources involved in sulphide mineralization.

## 1. Introduction

The Phalaborwa phoscorite-carbonatite Complex (PC) in the Limpopo Province of South Africa is an unique intrusion for several reasons. It is one of the most ancient carbonatites worldwide (Woolley and Kjarsgaard, 2008) and the oldest known on the southern African continent. It is formed by a spatial association of phoscorite - a rare and conspicuous coarse-grained ultramafic rock, carbonatites, and pyroxenites, all of which are enveloped by a zone of metasomatism (fenitization) along the contact with the Archaean gneissic and granitic country rocks. The PC is the only known carbonatite to host an economic Cu deposit, and also contains world-class deposits of other materials, such as apatite and vermiculite, with significant by-products of magnetite, uranothorianite, baddeleyite, rare earth elements, nickel, gold, silver, and platinum-group elements (e.g.,Verwoerd and Du Toit, 2006).

Petrologic models for carbonatite genesis (e.g., Bell & Simonetti, 2008; Fischer et al., 2009; Sasada et al., 1997) require metasomatized lithospheric and asthenospheric mantle sources. Generally, high abundances of incompatible elements, including those responsible for heat production (U, Th, and K), as well as alkali-earths (Cs, Rb, and Ba) are consistent with small degree partial melting. Three main mechanisms include: (i) partial melting of a carbonate-rich peridotite or wehrlite (e.g., Dalton and Wood, 1993), (ii) fractional crystallization from an alkaline silicate melt (e.g., Veksler et al.,

1998) or a Fe–P–Si-rich melt (e.g., Krasnova et al., 2004a), and (iii) carbonate–silicate magma immiscibility (e.g., Lee and Wyllie, 1998). However, details of their petrogenesis are often shrouded in uncertainty, such as the genetic relationship among compositionally and mineralogically distinct rock types.

Despite its significant Cu-sulphide mineralization, only a single study has examined the sulfur isotope composition of the PC (Mitchell and Krouse, 1975), and no study as yet has attempted to utilize multiple S isotope ratios integrated with Pb isotope values as tracers for mantle and crustal contribution. Recent studies have documented the presence of surface-derived sulphur with a mass-independent S isotope signature (MIF-S) within mantle-derived rocks. Production of MIF-S (defined by $\Delta^{33}S = \delta^{33}S–[(1+\delta^{34}S)^{0.515}-1]\times1000 \neq 0.0$ ‰ or $\delta^{34}S/\delta^{33}S$ ratios significantly outside of the 0.500-0.520 range) occurred prior to the Great Oxidation Event (GOE) at ca. 2.4 Ga due to photochemical reactions in an Archaean oxygen-poor atmosphere (e.g., Farquhar et al., 2000; Bekker et al., 2004). For instance, sulphide inclusions in eclogitic diamonds (e.g., Farquhar et al., 2002; Thomassot et al., 2009) and olivine-hosted sulphide inclusions from the islands of Mangaia (Cabral et al., 2013) and Pitcairn (Delavault et al., 2016) show non-zero $\Delta^{33}S$ values, which were interpreted to reflect subduction and storage of hydrothermally altered Archaean oceanic crust and marine sediments deep in the mantle. However, most mantle-derived oceanic magmatic rocks do not record anomalous S isotope compositions, e.g., ocean island basalts from the island of Samoa (Labidi et al., 2013, 2015). Most recently, Magalhães et al. (2018) reported MIF-S for sulphides from several stratigraphic horizons within the Bushveld Complex (BC) – the world's largest layered mafic intrusion. The emplacement of the BC may have involved crust-contaminated, mantle-derived melts (e.g., Wilson, 2012), possibly with the sulphur being sourced at

depth, instead of being assimiliated from upper crust (Magalhães et al., 2019). Given the growing number of reported cases of mantle-derived rocks containing a recycled ancient sulfur signature and the possibility that the Bushveld and Phalaborwa complexes formed during a common, large-scale magmatic event, the present study was designed with the following aims:

- To analyze multiple S isotopes in sulphides at high spatial resolution in in search of a pre-GOE surface-derived component;
- to obtain Pb isotope ratios, coupled with S isotopic data, for individual sulphides in an attempt to date the timing of mineralization and to constrain possible crustal contribution;
- to compare new and published isotopic data to assess whether the Bushveld and Phalaborwa complexes might be genetically linked and, specifically, if S-bearing fluids/melts shared a common source, and
- to evaluate the respective contribution from asthenospheric and lithospheric (including supracrustal) sources during carbonatite magmatism at ca. 2.06 Ga.

Lead and multiple sulphur isotope data were also evaluated in the light of textural characteristics of sulphide mineralization and whole-rock trace element geochemistry.

## 2. Geology

The Phalaborwa Complex forms a lobate-shaped, ultramafic to alkaline intrusion measuring 7 km in N–S and 3.2 km in W– E direction (Figs. 1A, B; e.g., Verwoerd and Du Toit, 2006). Intruded into >2.9 Ga granite and gneisses of the Kaapvaal Craton (KC), the complex is composed of three overlapping pipe-shaped intrusions, each concentrically zoned (Figs. 1B, C). The architecture of the complex is similar to

the Alnö carbonatite ring-complex of central Sweden that has been related to caldera-type volcanism (Andersson et al., 2013). The main rock is mica-rich pyroxenite (bearing diopside, phlogopite, and apatite), grading into feldspathic pyroxenite at the contact with country rock and locally developed fenitization. Irregularly distributed syenite bodies mark the contact of the granite-gneiss basement with the pyroxenite, extending over several kilometers (Eriksson, 1989). In the central and southern pipes, ultramafic pegmatoids consist mostly of phlogopite, apatite, and clinopyroxene. The central pipe (Loolekop), some 0.8 km (N–S) by 1.4 km (W–E) in size, is the focus of this study (Figs. 1C, D). Here, the pegmatoidal rocks have been intruded by phoscorite and then carbonatite, the latter containing most of the copper mineralization (Figs. 1C, D; Lombard et al., 1964).

Phoscorite is a rare ultramafic rock mainly formed by olivine (often serpentinized), apatite, magnetite, phlogopite, and minor calcite. Phoscorite commonly occurs in association with carbonatite to form a phoscorite–carbonatite series (e.g., Krasnova et al., 2004b). At Phalaborwa, this rock type is coarse-grained and often shows a distinct banding defined by magnetite aggregates and clots parallel to the pipe margins (e.g., Milani et al., 2017a). The phoscorite has either sharp or gradational contacts with the banded carbonatite, corresponding to the older emplacement event. The banded carbonatite, having both fine- and coarse-grained varieties, is composed of Mg-rich calcite, displaying exsolution lamellae of dolomite (e.g. Milani et al., 2017b), magnetite, and apatite, with minor phlogopite, chondrodite, and rare olivine components (Eriksson, 1989). Layers of magnetite clots and phlogopite streaks constitute a prominent, but discontinuous foliation, parallel to the phoscorite banding, interpreted as a flow texture because it is commonly deflected around large mineral grains (Lombaard et al., 1964). A finer banding, due to

preferential orientation of small magnetite, apatite, and silicate grains, also exists. Originally interpreted by Lombaard et al. (1964) as a younger, superimposed structure, the banding has been subsequently related to the first, main magmatic event. The final intrusive phase utilized a stockwork of fractures at the time when igneous activity was renewed and formed a pipe-centered swarm of discontinuous carbonatite veinlets, called the transgressive carbonatite, which shows no banding, cuts across the banded carbonatite and other rock types, and hosts most of the copper mineralization (Fig. 1D). This late-stage carbonatite consists of calcite with abundant dolomite, apatite, phlogopite, magnetite, and sulphides. A suite of NE–SW-trending gabbro dykes intruded shortly after the main intrusive phase (Wu et al., 2011) all the rocks of the Loolekop pipe (Figs. 1C, D). Geochronological data for the complex are summarized in Wu et al. (2011), including ages for coexisting zircon and baddeleyite from all the diverse rock types within the complex (pyroxenite, phoscorite, banded and transgressive carbonatite, syenite, and dolerite dyke). U-Pb zircon ages suggest that the PC was emplaced at 2060 ± 2 Ma (Wu et al., 2011), thus slightly pre-dating the BC with an age of 2055-2056 Ma (Zeh et al., 2015).

## 3. Petrography

Considered late-stage products in the crystallization sequence, the copper sulphides in the Loolekop pipe have been assigned to three main stages of mineralization (Wilson, 1998). A summary of observed sulphide minerals, their textures, and assignment to mineralisation stage is provided in Table 1. The first stage produced both phoscorite and carbonatite, with bornite and chalcocite developed as disseminated grains, small droplets, and larger aggregates with magnetite, apatite, and mica, or lenses parallel to the magnetite banding. Bornite sometimes replaces calcite,

and both bornite and chalcopyrite occur as inclusions in pyroxenes (Figs. 2A, B), and contain inclusions of olivine (Eriksson, 1989). Within banded carbonatite, bornite is also the main sulphide and is observed to occur as disseminated grains, inclusions within olivine, magnetite, and calcite and patches/lenses parallel to bands with silicates and phosphates (e.g., Viereicher et al., 2000).

The first stage was followed by the main mineralization event that produced bornite, chalcopyrite, and minor pyrite, pyrrhotite, and cubanite (Fig. 2C), mainly within the transgressive carbonatite. Cu concentration is ~2-3 wt%, and sulphides are found preferentially along fractures, which acted as channels for ore-bearing fluids (Fig. 2D). The mineralized veins are centimeter-wide and up to a few meters long, and either define an irregular network or are aligned along several fracture systems, locally resulting in a distinct foliation within the host rock. On cooling, bornite commonly exsolved first chalcopyrite and then chalcocite (Fig. 2E) with chalcocite locally developing myrmekite-like pattern in bornite (Fig. 2F). The final stage in mineralization happened at lower temperature and resulted in a stockwork of cross-cutting veins filled with predominantly chalcocite and valleriite (Figs. 2G, H). The latter appears mainly associated with shearing that cross-cut older fractures. Sulphides of this stage are seen to replace all the main mineral phases and are often developed as rims on chalcopyrite and bornite. Other less common sulphides at Phalaborwa include covellite, tetrahedrite, linnaeite, marcasite, molybdnenite, sphalerite, galena, and Ni-sulphides such as bravoite, millerite, pentlandite, and violarite (e.g., Verwoerd 1986).

Temperature estimates based on geothermometry range from 150 to 800°C (for non-sulphides), and up to 1000°C (for sulphides) (Eriksson, 1989). Rudashevsky et al. (2004) also obtained temperatures in the range of 80 – 480°C (using PGE minerals). Other estimates suggest temperatures from 675°C (calcite-dolomite solvus for

carbonatite; Verwoerd, 2006) to 600°C (sulphide-phase stability; Hanekom et al., 1965). Considering that Na-carbonatites can erupt at temperature of 500 to 600°C (Weidendorfer et al., 2017), temperatures above 500°C would suggest that most sulphides (except valleriite) formed under magmatic conditions, consistent with the assertion by Vielreicher et al. (2000) that "ore fluids were high temperature, highly saline, $CO_2$-rich and magmatic water dominated chloride brines." The latter study also suggests that valleriite precipitated from meteoric water-dominated fluids.

## 4. Methods and samples

Isotope ratio measurements were carried out sequentially in three separate labs (NordSIMS: Swedish Museum of Natural History, stable isotope laboratories at the University of Maryland, and the University of Queensland), adopting three analytical techniques to obtain S and Pb isotopic data. Analytical details are provided as supplementary material (SM1: In-situ Pb isotope ratio measurements of sulphides by SIMS; SM2: In-situ S isotope ratio measurements of sulphides by SIMS; SM3: S isotope ratio measurements with the $SF_6$ method using a fluorination line coupled to a DI-IRMS; SM4: S isotope ratio measurements with the SO-$SO_2$ method using an elemental analyzer coupled to a continuous-flow isotope-ratio mass-spectrometer (EA-CF-IRMS)).

Initially, Pb ($^{206}Pb/^{204}Pb$, $^{207}Pb/^{204}Pb$, $^{208}Pb/^{204}Pb$) and S ($^{33}S/^{32}S$, $^{34}S/^{32}S$) isotope ratios were measured in-situ using thin sections of six drill core samples, comprising two phoscorites (B66, GC813C1), two banded carbonatites (B67, GC813A2), and two transgressive carbonatites (B61B, B62E) (Table 2). Analyzed sulphide minerals include bornite, chalcocite, chalcopyrite, cubanite, and valleriite (Fig. 3). Lead and S isotope data were acquired on the same sulphide grains, resulting in coupled Pb and S

isotope data at high spatial resolution. For Pb isotope ratio measurements, instrument mass fractionation (IMF) by SIMS is relatively small (Shimizu and Hart, 1982) and, for analysis of the low-Pb sulphides in this study, is entirely encompassed by uncertainties on the measurement. For S isotopes, IMF is strongly influenced by mineral composition and, in some cases, crystallographic orientation (e.g., Huberty et al., 2010), and accurate determination of S isotope ratios requires compositionally matched reference materials. For example, calibration of $\delta^{34}S$ values in pyrrhotite using a pyrite reference material will yield values approximately 3 ‰ lighter. In the present study, only chalcopyrite had a compositionally matched reference material and therefore $\delta^{34}S$ values for other sulphide phases are likely inaccurate by up to several permil (Whitehouse, 2013). In contrast to S isotope ratios, determination of the mass-independent fractionation, expressed as $\Delta^{33}S$, is not compositionally controlled, and these values are accurate at the precision level stated.

In order to validate SIMS S isotope data and obtain information on all sulphur isotopes, S was extracted from bulk-rock samples hosting the sulphides and subjected to isotope ratio analysis at the University of Maryland (SM3). This dataset consequently represents average isotope composition of sulphide minerals in silicate and carbonate matrices, and comprises all three S isotope ratios ($^{33}S/^{32}S$, $^{34}S/^{32}S$, and $^{36}S/^{32}S$; Table 2), but without spatial resolution and distinction among sulphide minerals. Sulfur isotopic compositions are reported using the delta ($\delta$) notation with respect to the Vienna Canyon Diablo Troilite (V-CDT) standard. This results in -0.394 ‰, 0.116 ‰, and -0.795 ‰ values for the $\delta^{34}S$, $\Delta^{33}S$, and $\Delta^{36}S$ of the IAEA-S1 standard as published in Dottin et al. (2018). Variations in mass-independent fractionation were quantified using $\Delta^{33}S = \delta^{33}S - [(1 + \delta^{34}S)^{0.515} - 1] \times 1000$. Finally, sulphide mineral separates were obtained from phoscorite (chalcopyrite), banded

carbonatite (chalcopyrite and bornite), and transgressive carbonatite (chalcopyrite and bornite) host rocks by micro-drilling, and ~50 mg of powder were subjected to continuous flow isotope-ratio mass-spectrometry to measure $\delta^{33}S$ and $\delta^{34}S$ (Table 2), thereby retaining some mineralogical information. Analytical data are listed in tables of the supplementary material (SM Tables 1, 2, 3).

Representative trace element compositions for all three major rock types (phoscorite, banded and transgressive carbonatites) were obtained for drill core samples several centimeter thick to minimize sampling bias and to avoid oversampling of accessory minerals that could be enriched in some trace elements. Minor and trace element concentrations of whole-rock samples were determined by solution-based ICP-MS analysis at the Earthlab within the School of Geosciences, University of the Witwatersrand. Analytical details are provided in the supplementary material (SM5: ICP-MS (solution) measurements of trace elements for whole rocks), and the data are listed in the supplementary material (SM Table 4), including measured values for the International Certified Reference Materials BHVO-2 and BCR-2.

## 5. Results

### *5.1. Whole-rock trace-element geochemistry*

Trace-element compositions (normalized to Primitive Mantle: PRIMA) are shown in Fig. 4, and represent averages for individual analyses. The patterns for all rock types are remarkably similar, displaying depletion in the most incompatible and mobile elements (Cs and Rb), elevated concentrations of incompatible elements (La to Gd and U), significant negative anomalies for some HFSE (Nb, Ta, Zr, and Hf), mild relative depletions of Sr and Eu, and anomalously low Pb concentrations (compared

to neighboring elements Ce and Pr).

### ***5.2.*** *Lead isotope data*

Lead isotope data for individual sulphides from the PC are displayed in diagrams of $^{207}Pb/^{206}Pb$ vs. $^{204}Pb/^{206}Pb$ (Fig. 5A) and $^{207}Pb/^{204}Pb$ vs. $^{206}Pb/^{204}Pb$ (Fig. 5B), including data for sulphides from the Upper Critical Zone of the Bushveld Complex (Mathez and Waight, 2002). Isotope evolution curves for three hypothetical terrestrial reservoirs are also shown, namely upper continental crust, MORB mantle (Kramers and Tolstikhin, 1997), and undepleted mantle (Kamber and Collerson, 1999). Systematic Pb isotope variations are observed for individual rock types, although ranges for each rock type are small (<1.4 for $^{206}Pb/^{204}Pb$), except for one phoscorite sample B66 (excluding one very radiogenic analysis, its $^{206}Pb/^{204}Pb$ range is 66).

### *5.3. Sulphur isotope data*

Sulphur isotope data obtained by SIMS for individual sulphide phases are shown in diagrams of $\delta^{33}S$ vs. $\delta^{34}S$ (Fig. 6A) and $\Delta^{33}S$ vs. $\delta^{34}S$ (Fig. 6C). Values for $\delta^{34}S$ span a wide range from -15 to +15 ‰, which cannot be explained by IMF related to compositional differences between samples and reference materials. A small fraction of all the data fall within the range typical for mantle sulphides. The range in $\delta^{34}S$ values from -1.61 to -0.95 ‰ reflects the S isotope composition of unmodified MORB mantle and OIBs without a recycled crustal component (Labidi et al., 2013). Only six SIMS data overlap with the narrow range of the expected $\Delta^{33}S$ composition of the mantle (0.006 ± 0.008 ‰; Labidi and Cartigny, 2016). Instead, the majority of SIMS analyses yielded $\Delta^{33}S$ values of -0.4 to +0.8 ‰, well outside of the mantle range.

Isotope data for whole-rock samples and sulphide mineral separates (Figs. 6B and 6D) display a much smaller range of $\delta^{34}S$ compositions (-0.6 to +2.6 ‰) and only positive $\Delta^{33}S$ values (+0.2 to +0.7 ‰). Half of this data overlaps with the range of $\delta^{34}S$ composition of the mantle (Fig. 6B), and also confirms the MIF-S observed in the SIMS data.

The $\Delta^{33}S$ vs. $\Delta^{36}S$ graph (Fig. 6E) shows that the PC sulfur isotope data plot along the mass-independent fractionation array of Archaean sediments (cf. Farquhar et al., 2007). The S isotope composition of the PC overlaps with the wide range in $\delta^{34}S$ and $\Delta^{33}S$ values observed for the Transvaal Supergroup strata (except for valleriite data; Fig. 6C), but is distinct from the previously obtained data for the Bushveld Complex sulphides (Figs. 6C, D). Coupled S and Pb isotope data are shown in Fig. 6F. An offset from the isochron ($\Delta^{207}Pb/^{206}Pb$) is calculated as a difference in $^{207}Pb/^{204}Pb$ values for isochron and measured sulphide at a given $^{206}Pb/^{204}Pb$ value, divided by the measured value, and expressed in %. Positive values for the offset indicate position of Pb isotope data above the isochron.

## 6. Discussion

### *6.1. Timing of Mineralization and Source(s) of Pb*

In $^{207}Pb/^{206}Pb$ vs. $^{204}Pb/^{206}Pb$ space, sulphide data are tightly clustered along a regression line. Two approaches were adopted to calculate model ages. In model 1, data points are weighted according to the respective errors (Ludwig, 2008). Since the probability of fit was <15 %, 95% confidence errors were calculated (cf. Ludwig, 2008). The model 1 apparent age is 1935 ± 39 Ma. Model 2 on the other hand assumes zero error correlations and assigns equal weight to each data point (Ludwig, 2008), returning an apparent age of 2054 ± 99 Ma. In both cases the MSWD of 2.4 is

just slightly higher than unity and therefore suggests that the scatter is largely due to analytical uncertainty. While the total error associated with model 1 age is smaller than that in model 2, the latter agrees (within error) with the constrained emplacement age for the PC: 2060 ± 4 Ma (pyroxenite), 2062 ± 2 Ma (phoscorite), 2060 ± 2 Ma (banded carbonatite), and 2057 ± 3 Ma and 2060 ± 1 Ma (transgressive carbonatite) (all error weighted mean $^{207}Pb/^{206}Pb$ dates for zircon and baddeleyite; Wu et al., 2011). Based on the agreement with the robust and precise U-Pb zircon and baddeleyite ages, the model 2 age is inferred to indicate the age of sulphide mineralisation. Alternatively, the model 1 age of ~1935 Ma might reflect a geologically significant event in the region rather than analytical error. This is best illustrated through comparison with timing of the mafic intrusive events of the Bushveld Complex. Although the primary, magmatic age for this intrusive event is precisely constrained between 2056 and 2053 Ma with U-Pb zircon dates (Zeh et al., 2014; Scoates and Wall, 2017), indicating rapid cooling below zircon closure temperature, the growing age database also indicates protracted cooling and late disturbance. For instance, while detailed geochronology of the mineralized Merensky Reef shows that rapid crystallization occurred between 2055 and 2050 Ma, slow cooling and a hydrothermal resetting event as young as ~1980 Ma are recorded by U-Pb apatite and Ar-Ar biotite dates (Scoates and Wall, 2017). It is thus possible that the 1935 ± 39 Ma date registered by the Model 1 Pb-Pb age reflects hydrothermal disturbance in the system. A possible cause of the disturbance might relate to metamorphic and deformation events in the Central Zone of the Limpopo Orogen (Kramers and Mouri, 2011).

In order to determine the source of sulphidic lead, Phalaborwa data are considered within the framework of terrestrial Pb isotope models (Fig. 5B). In the $^{206}Pb/^{204}Pb$ vs.

$^{207}Pb/^{204}Pb$ isotope space the data define an array that corresponds to the age of the PC (ca. 2.06 Ga). The linear regression does not project to MORB mantle, undepleted mantle or average Archaean lower continental crust, but instead intersects the upper continental crust growth curve at 2.4-2.5 Ga and a hypothetical mixing line between MORB mantle and the continental crust at 2.06 Ga. Three inferences regarding the potential source for Phalaborwa sulphide Pb can be made: (i) Lead was not exclusively sourced from the MORB mantle at 2.06 Ga; (ii) lead represents a mixture of evolved and MORB-like mantle Pb, with geometric relationships suggesting >50% of an evolved component, such as supracrustal material or enriched subcontinental lithosphere; (iii) if lead was solely derived from the crust then intersection with the Pb growth curve requires this material to be formed before ca. 2.4 Ga, a condition consistent with the observed MIF-S (see below).

Both the magnitude of $\Delta^{33}S$ signal and the offset of Pb data from the regression line ($\Delta^{207}Pb/^{204}Pb$; Fig. 6F) may serve as non-quantitative proxies for the amount and nature of pre-2.4 Ga supracrustal material incorporated into mantle-derived melt. However, no simple picture unfolds when $\Delta^{207}Pb/^{204}Pb$ and $\Delta^{33}S$ signals are compared, possibly because Pb isotopes convey information on magmatic and metamorphic evolution of the lithosphere, whereas S isotopes register atmospheric processes subsequently diluted by mixing with mantle and crustal sources and high-temperature processing. A few data points with $\Delta^{207}Pb/^{204}Pb \sim 0$ correspond to $\Delta^{33}S \sim 0$ ‰, and almost all negative $\Delta^{207}Pb/^{204}Pb$ values show positive $\Delta^{33}S$ compositions, while an equal number of data points have both negative and positive MIF-S signals at positive $\Delta^{207}Pb/^{204}Pb$ values (Fig. 6F). Valleriites from phoscorite and transgressive carbonatite have highly positive $\Delta^{33}S$ values and both negative and positive $\Delta^{207}Pb/^{204}Pb$ compositions. When considered separately, a negative correlation,

although poorly developed, is discernible for phoscorites and banded carbonatites (Fig. 6F).

Considering the different generations of sulphides and the Pb and S isotope heterogeneity, we infer that both Pb and S were sourced from multiple reservoirs, without subsequent homogenization at any stage. Therefore, partial melting of an asthenospheric mantle source that incorporated subducted supracrustal material and subsequent melt extraction, as well as effective convective mixing of ponding magma in a chamber appear unlikely as all of those processes would have created more homogeneous isotope compositions. The ascending magma may have interacted on the way with, and assimilated, heterogeneous material, including supracrustal materials or metasomatized sublithospheric mantle, after being extracted from the mantle source.

*6.2. Sulphur isotope variability – assessing magmatic vs. hydrothermal signatures*

Interpretation of Pb and S isotope data requires establishing which sulphides formed earlier from magmas and later from hydrothermal fluids. Early sulphides would likely have derived their S and Pb isotope compositions from melts and magmatic fluids and therefore carry information on magmatic sources, whereas late sulphides may have been in equilibrium with fluids that interacted with country rocks and thus obtained signatures of near-surface reservoirs.

Petrographic observations coupled with thermometry suggest that bornite and chalcocite in phoscorite and banded carbonatite likely precipitated under magmatic conditions, whereas bornite in transgressive carbonatite possibly formed from hydrothermal fluids (Table 1). Valleriite as a very late stage product precipitated hydrothermally and likely would represent a crustal signature. Chalcopyrite may be

transitional between two modes of emplacement. A magmatic origin for bornite and chalcopyrite is inferred from mingling textures of transgressive, oxidized carbonatite melt and Cu-sulphide-bearing, reduced melt, implying a magmatic origin for Cu and associated S and Pb (Kavecsanszki et al., 2014).

Two SIMS analyses of magmatic bornite in phoscorite yield $\delta^{34}S$ and $\Delta^{33}S$ values that straddle the mantle range, while one other data point has $\Delta^{33}S \sim +0.45 \pm 0.11$ ‰ with $\delta^{34}S$ value just below the mantle range. Chalcocite in phoscorite shows a larger spread in $\delta^{34}S$ values outside the mantle range, with one out of three data points having $\Delta^{33}S$ composition of $+0.75 \pm 0.38$ ‰. Five out of six bornite analyses from banded carbonatite have mantle $\delta^{34}S$ values with resolvable MIF-S signal ($\Delta^{33}S$ from $+0.58 \pm 0.12$ to $1.00 \pm 0.09$ ‰). Two chalcocite analyses have highly negative $\delta^{34}S$ values of -9 and -14 ‰ with $\Delta^{33}S$ values +0.5 and +0.7 ‰. Valleriite from phoscorite and transgressive carbonatites shows the most extreme $\Delta^{33}S$ values, up to +2.5 ‰, and $\delta^{34}S$ values < -5 ‰. The majority of sulphide data, including those for pyrite and chalcopyrite, have mantle $\delta^{34}S$ values and resolvable MIF-S signal with both positive and negative signs. Considering SIMS data alone (Fig. 7A), $\Delta^{33}S$ values for transgressive and banded carbonatites are clearly different, while the spread in $\Delta^{33}S$ values for phoscorite encompasses the range defined by both types of carbonatites. Bornites from all rock types combined display the largest range in $\Delta^{33}S$ values, from less than 0 to above 1 ‰ (Fig. 7B). The range of the S isotope data of sulphide mineral separates and whole-rock analyses is much more restricted relative to SIMS analyses. Approximately 80% of the data fall outside the mantle range ($\delta^{34}S$ between -1.61 and -0.95 ‰), and in addition most of the data are mass-independently fractionated ($\Delta^{33}S \neq 0.000 \pm 0.008$ ‰ at $2\sigma$ uncertainty). In summary, SIMS, EA-

CF-IRMS, and DI-IRMS data show a ubiquitous MIF-S signature, with the larger spread in $\Delta^{33}S$ and $\delta^{34}S$ values in *in-situ* mineral analysis by SIMS. Significant sulphur isotope heterogeneity is present on a small scale even between different crystals of the same mineral in the same host rocks (e.g., bornite in banded carbonatite, Fig. 6C). It is possible that some sulphides, such as valleriite, incorporated S and Pb from migrating fluids that had exchanged with extraneous materials, including host rocks to the intrusion, during post-magmatic hydrothermal activity. Importantly, sulphides of likely magmatic or magmatic-hydrothermal origin (e.g., bornite) carry MIF-S signal. At the same time, even sulphides with a low-temperature, hydrothermal origin could have entrained S and Pb from magmatic sources, if these fluids were largely of magmatic origin (cf. Vielreicher et al., 2000). Sulphur with $\delta^{34}S$ values of –2 to 0 ‰ at the PC was interpreted to be of mantle origin, while ratios up to +5 ‰ were previously attributed to contamination with crustal sulphate (Mitchell and Krouse, 1975).

### *6.3. Surface-derived sulphur: Source(s) and mechanisms for incorporation*

#### *6.3.1. Crustal contamination at shallow level*

Based on the ubiquitous MIF-S signature in sulphides and host rocks across all sulphide species and rock types (phoscorite and carbonatites), assimilation of supracrustal materials at shallow crustal levels, either during magma ascent or ponding at middle to upper crustal levels, seems likely. Incorporation of sedimentary material from the Transvaal Supergroup is further suggested by the similarity in $\Delta^{33}S$ and $\delta^{34}S$ values for sulphides from the Transvaal Supergroup and the PC (Figs. 6C, D). A crustal S isotope signature would be more likely to be strongly imparted on sulphides that formed late as fluid circulation during hydrothermal activity could have

reached to supracrustal materials surrounding the PC. However, a systematic relationship of S isotope ratios as a function of rock type (phoscorite was emplaced before carbonatites) or sulphide species (bornite formed early during magmatic crystallization, whereas valleriite formed late within fractures cross-cutting solidified intrusion) is not observed.

Crustal contamination of mantle-derived rocks can be evaluated using whole-rock trace element compositions normalized to Primitive Mantle (Fig. 4). Elevated incompatible trace element concentrations and negative Pb anomalies resemble those in magmas derived from enriched mantle plumes (EM, HIMU; e.g., Hofmann, 1997). Negative HFSE anomalies are indicative of the subcontinental lithospheric mantle (SCLM) that was metasomatized by melts/fluids derived from subducting plate (e.g., Kalfoun et al., 2002). Since continental crust is largely formed via subduction magmatism (e.g., Rudnick, 1995), depleted HFSE compositions are also imparted onto sedimentary rocks, hindering the distinction between a primary subduction signature and incorporation of crustal material into mantle-derived magmas. The hallmark of the continental crust composition – a proxy to surface-derived sedimentary material that may have provided MIF-S signature to the PC sulphides – are Ce/Pb ratios that are lower than values for OIB and MORB (~25). In contrast, all three rock types of the PC show anomalously low Pb concentrations, with Ce/Pb ratios of 100 to 240, entirely inconsistent with crustal contamination. Likewise, Nb/U values (<1) are consistently below continental crust and arc values (Nb/U~10) as well as those of asthenospheric mantle-derived rocks (~47) (e.g., Hofmann, 1997), ruling out an exclusive origin of the PC rocks from unmodified mantle sources. Interpretation of carbonatite petrogenesis is complicated and beyond the scope of the study. Irrespectively, PRIMA-normalized compositions display similarities to OIBs

and negate significant crustal material assimilation during emplacement. Specifically, strong HFSE anomalies, coupled with the absence of crustal Pb enrichment, argue against assimilation of upper crustal materials after magma extraction from the asthenosphere, but suggest that carbonatite-phoscorite melts interacted with, or incorporated, a component from SCLM.

Involvement of SCLM in the petrogenesis of the near-coeval, ca. 2055 Ma Bushveld Complex (BC) was proposed in several studies, using a variety of geochemical datasets (e.g., Richardson and Shirey, 2008; Zirakparvar et al., 2014). Considering that both Phalaborwa and Bushveld magmas have traversed the SCLM underlying the Kaapvaal Craton (KC), insights from the BC should be helpful to understand whether the PC magmas were affected by, or interacted with, the KC lithospheric mantle. Penniston-Dorland et al. (2012) observed that sulphides of the Main and Critical zones of the BC display laterally homogeneous, non-zero $\Delta^{33}S$ values, in contrast to variable whole-rock radiogenic isotope compositions. They suggested that the magma carried a homogeneous MIF-S signature prior to the BC emplacement at shallow crustal levels. In a follow-up study by Magalhães et al. (2018), using an extended S isotope dataset, contribution from lithospheric mantle was considered plausible, but it was also argued that multiple sources could have contributed to the magmatic system of the BC. Magalhães et al. (2019) proposed that the upper continental crust is not the source of sulphur for the BC, further implying a possible mantle source for the anomalous sulphur signature. With respect to the PC, several studies suggested involvement of lithospheric mantle. For instance, Kavecsanszki et al. (2014) proposed that compositionally distinct magma types, including ultramafic silicate melts from the deep mantle, and carbonatitic oxidized melts from metasomatized mantle, possibly the SCLM, mingled, mixed, and

underwent complex igneous fractionation to produce the lithological varieties of the PC. On the basis of radiogenic Sr and unradiogenic Nd-Hf isotope compositions of apatite and zircon, Wu et al. (2011) argued that an enriched mantle plume impinged on, and caused partial melting of, the SCLM underlying the KC. Considering that sulphides are mostly magmatic or magmatic-hydrothermal in origin (see above), it would therefore appear most likely that sulphidic xenomelts were also derived from asthenospheric and sub-continental lithospheric mantle reservoirs. The question remains how a MIF-S signature was derived from these mantle sources? Several studies documented events that caused partial melting and metasomatism of the SCLM underlying the KC (e.g., Richardson and Shirey, 2008). Mantle metasomatism is ascribed to subduction-related element transfer from oceanic slab and overlying sediments; a process by which a characteristic subduction signature, such as HFSE anomalies displayed by carbonatites and phoscorite from the PC (Fig. 4), could have been imprinted. Evidence for fluid-induced, metasomatic alteration with sulphate-bearing fluid of the Kaapvaal cratonic lithospheric mantle was recently documented in xenoliths of the Bultfontein kimberlite (Guliani et al., 2013). Dehydration and partial melting of oceanic slab and overlying sediments could have transported MIF-S and isotopically evolved Pb to the SCLM. Critically, a fundamental link between metasomatism of the Kaapvaal SCLM and MIF-S signature was indeed demonstrated with diamond-hosted sulphide inclusions within the Orapa and Jwaneng kimberlites on the periphery of the KC, which carry supracrustal isotope signatures, with values of $\Delta^{33}S$ ranging from -0.5 to +0.9 ‰ (e.g., Thomassot et al., 2009). These findings strengthen the notion that sulphide mineralization of the PC can be linked to the SCLM underneath the KC.

*6.3.2. Recycling into an asthenospheric mantle source?*

Several observations suggest that melts, which formed the Phalaborwa carbonatite-phoscorite intrusion were, at least in part, derived from the asthenospheric portion of the mantle. Whole-rock normalized trace element compositions show similarity with plume-derived magmas with an enriched mantle signature (Fig. 4), specifically the negative Pb anomaly and abundances of incompatible elements in the range of 1000 x Primitive Mantle. Likewise, carbon isotope systematics of the Phalaborwa carbonatite is consistent with a mantle source for carbon (Horstmann and Verwoerd, 1997).

In their compilation of sulphur isotope composition of carbonatites, Mitchell and Krouse (1975) inferred that Phalaborwa igneous rocks have $\delta^{34}S$ values compatible with an asthenospheric mantle source. Assuming that $\delta^{34}S$ values of -1.28 ± 0.33 ‰ represent unmodified MORB and OIB mantle sources without any contribution of recycled crustal component, such as hydrated oceanic crust or oceanic sediments (Labidi et al., 2013), six data points from the PC may reflect derivation from asthenospheric mantle source. However, among these sulphides, all except for one still show resolvable, non-zero MIF-S signature. Recycled supracrustal components have been inferred as a sulphur source for sulphide inclusions in eclogitic diamonds (e.g., Farquhar et al., 2002; Thomassot et al., 2009), several OIBs fed by mantle plumes (Cabral et al., 2013; Delavault et al., 2016), and magmas derived from the sub-arc mantle wedge (e.g. Aoyama et al., 2018). Therefore, the possibility exists that subduction of pre-GOE, sulphur-bearing oceanic lithosphere and sediments generated a reservoir with MIF-S signature and radiogenic Pb isotope characteristics that served as an asthenospheric source for the PC. The wide range in S isotope composition of Phalaborwa sulphides, especially seen in SIMS analyses, requires heterogeneous supracrustal material in the magma source. A potential issue with this requirement is

that the relatively large variability in $\Delta^{33}S$ and $\delta^{34}S$ values seems to conflict with mixing and homogenization expected during prolonged storage in a convecting mantle regime. However, sulphur isotope data for olivine-hosted sulphides in modern OIBs also display a certain degree of variability on Mangaia, Cook Islands ($\Delta^{33}S$ = +0.03 ± 0.28 to -0.49 ± 0.26 ‰, $\delta^{34}S$ = -5.92 ± 1.27 to -17.25 ± 0.61 ‰; Cabral et al., 2013) and Pitcairn Island ($\Delta^{33}S$ = +0.12 ± 0.14 to -0.85 ± 0.13 ‰, $\delta^{34}S$ = -2.27 ± 0.14 to -6.20 ± 0.25 ‰; Delavault et al., 2016). This highlights the possibility that pre-2.4 Ga supracrustal material could have preserved multiple S isotope heterogeneity despite extended residence time in the hot and convecting mantle before incorporation into a mantle plume and resurfacing.

*6.4. Isotope perspective on a relationship with the Bushveld Complex*

Subcontinental lithospheric and asthenospheric mantle contributions are often implicated in the origin of carbonatites, with the temporal and petrogenetic association of carbonatites and Large Igneous Provinces (LIPs; Bell and Simonetti, 2010) arguing for a common mechanism involved. Within the South African context, this would be the Phalaborwa and Schiel carbonatites and Bushveld Complex – an array of large-scale fossilized magma chambers that form part of an ancient LIP on the African continent. The Rustenberg Layered Suite of the Busvheld Complex was emplaced between 2055.9 ± 0.3 Ma and 2054.9 ± 0.4 Ma (Zeh et al., 2015), while the emplacement of the PC occurred at around 2060 Ma. Given the broad similarity in the emplacement ages, both intrusive bodies could be the reflection of a mantle plume event. Zeh et al. (2015) inferred that large asthenospheric melt fluxes into the crust to form the Bushveld layered intrusion were caused by changes in the stress field within the SCLM. Vielreicher et al. (2000) inferred that volatile, $CO_2$-rich, oxidizing and

acidic metal-bearing fluids ultimately originated from decompressional melting of metasomatized SCLM. Considering a prominent role of lithospheric mantle contribution both complexes appear to have a shared petrogenetic history. Three isotope datasets are compared below to explore a possible petrogenetic link between the BC and PC, and to evaluate whether xenomelts involved in sulphide mineralization shared a common source at ca. 2.06 Ga.

Hf isotope data ($\varepsilon_{Hf}$) for zircons from the BC and PC are strikingly similar at 2.06 Ga: -9.0 to -6.8 (Zirakparvar et al., 2014) and -9.8 to -5.1, respectively (Wu et al., 2011). These values are significantly less radiogenic than the Depleted Mantle at the time of magmatism. In both cases, the small range of Hf composition was used to argue against shallow-level contamination by the continental crust, and in favor of models involving partial melting of SCLM by rising asthenospheric melts (Wu et al., 2011; Zirakparvar et al., 2014).

The most unradiogenic Pb isotope data for BC and PC sulphides occupy distinctly different regions in $^{206}Pb/^{204}Pb$ vs. $^{207}Pb/^{204}Pb$ space (Fig. 5B). Difference in Pb isotope composition might reflect either different timing of the source extraction from the mantle or their distinct U/Pb ratios (μ-values), or both. Mathez and Waight (2003) observed disequilibrium between feldspars and suphides in the BC, and argued for multiple Pb sources, including country rocks, and no faithful record of the composition of the primary magmatic sources. For reasons outlined above, we consider the Pb isotope data for the PC to be reliable and useful to infer source characteristics. Regardless of the petrogenetic significance of Pb isotope data, both sulphide datasets define distinct compositional arrays, and therefore imply that ore-mineralizing fluids did not share a common source of Pb.

Finally, while multiple S isotope data from both the PC (this study) and the BC

(Penniston-Dorland et al., 2012; Magalhães et al., 2018; 2019) display a resolvable MIF-S signal (Figs. 6C, D), several notable differences exist: (i) The range of S isotope values obtained by SIMS for the PC is considerably larger than that for the BC, (ii) the $\delta^{34}S$ values of sulphide mineral separates and whole rocks from the BC overlap with the SIMS data for the PC, but consistently show a smaller range in $\Delta^{33}S$ values, and (iii) importantly, in terms of $\Delta^{33}S$ values, datasets for the BC and PC are distinct and show no overlap (Fig. 6D).

Whereas an apparent isotope similarity between the BC and PC applies to zircon Hf isotope systematics, both lead and sulphur isotope data are resolvably different, requiring isotopically distinct sources for sulphide mineralization. Since PC magmatism preceded the formation of the BC, components of the SCLM with a lower melting temperature (more fertile with higher concentrations of incompatible elements) were probably initially mobilized and incorporated to a larger extent. With advanced impingement of the asthenospheric upwelling, contribution from heterogeneous SCLM diminished causing the temporal shift in S and Pb isotope systematics and decreasing S isotope variability.

## 7. Conclusions

Coupled Pb and multiple S isotope data for sulphide minerals from three principal host rock types (carbonatites and phoscorite) of the PC advance our understanding of timing and source of Cu mineralization, with implications for carbonatite petrogenesis and the genetic relationship to the BC. The following key observations and interpretations must be satisfied by any model for sulphide mineralization at the PC:

- Pb isotope data define a tightly clustered array corresponding to an age of 2054 ± 99 Ma.

- Pb isotope data indicate either a significant contribution from evolved (radiogenic) lithospheric material to asthenospheric mantle-derived melts or an "isotopically enriched", heterogeneous mantle source.
- SIMS sulphur isotope ratios for petrographically characterized sulphides show a large range in $\delta^{33}S$, $\delta^{34}S$, and $\Delta^{33}S$ values, with significant non-zero $\Delta^{33}S$ compositions. Sulphur isotope measurements of sulphide mineral separates and S extracts from whole rocks show smaller ranges, suggesting considerable isotope variation at the μm scale.
- Sulphur isotope data reveal resolvable and consistent MIF-S signature, irrespective of rock type and sulphide mineral, requiring the involvement of pre-2.4 Ga surface-derived materials.
- A lack of correlation between Pb and S isotope compositions points to independent Pb and S sources to form sulphides.
- Sulphides from the BC display Pb and S isotope compositions distinct from those observed for the sulphide mineralization of the PC.

The above observations are adequately explained by a model, whereby sulphides precipitated from xenomelt during main carbonatite-phoscorite emplacement. Sulphide xenomelt was predominantly derived from compositionally heterogeneous asthenospheric and lithospheric mantle, with minimal contribution from supracrustal sources at shallow crustal levels during magma emplacement.

**Acknowledgements**

This research was supported through funds (to RB) from the Faculty of Science, University of the Witwatersrand, and from the DST-NRF Centre of Excellence for

Integrated Mineral and Energy Resource Analysis (CIMERA) (to RB, LM, LLB). Participation by AB was supported by NSERC Discovery and Acceleration grants. Paulien Lourens and Thabitha Moyana from the Palabora Mining Company Ltd. (PMC) provided access to drill-core material, and their assistance is greatly acknowledged. NM thanks the Brazilian Government for a Science without Borders Fellowship (BEX1136-13-5). The authors would also like to thank Sarah Penniston-Dorland and James Farquhar for analytical and financial support. Sulfur isotope measurements conducted at University of Maryland were supported by NSF through the grant EAR-1551196 (SPD). Andrea Agangi is thanked for helpful comments. This publication is a contribution from NordSIMS, which is jointly operated by the Swedish Museum of Natural History, the Swedish Research Council and the University of Iceland. We appreciate editorial support by Rajdeep Dasgupta, and constructive criticism from Val Finlayson and one anonymous reviewer.

**References**

Andersson, M., Malehmir, A., Troll, V.R., Dehghannejad, M., Juhlin, C., Ask, M., 2013. Carbonatite ring-complexes explained by caldera-style volcanism. Sci. Rep. 3, 1677, 1-9.

Aoyama, S., Nishizawa, M., Miyazaki, J., Shibuya, T., Ueno, Y., Takai, K., 2018. Recycled Archean sulfur in the mantle wedge of the Mariana Forearc and microbial sulfate reduction within an extremely alkaline serpentine seamount. Earth Planet. Sci. Lett. 491, 109-120.

Bau, M., 1996. Controls on the fractionation of isovalent trace elements in magmatic and aqueous systems: evidence from Y/Ho, Zr/Hf, and lanthanide tetrad effect. Contrib. Mineral. Petrol. 123, 323-333.

Bekker, A., Holland, H.D., Wang, P.L., Rumble Iii, D., Stein, H.J., Hannah, J.L., Coetzee, L.L., Beukes, N.J., 2004. Dating the rise of atmospheric oxygen. Nature, 427, 117-120.

Bell, K., Simonetti, A., 2010. Source of parental melts to carbonatites–critical isotopic constraints. Mineral. Petrol. 98, 77-89.

Bolhar, R., Kamber, B.S., Collerson, K.D., 2007. U–Th–Pb fractionation in Archaean lower continental crust: Implications for terrestrial Pb isotope systematics. Earth Planet. Sci. Lett. 254, 127-145.

Cabral, R.A., Jackson, M.G., Rose-Koga, E.F., Koga, K.T., Whitehouse, M.J., Antonelli, M.A., Farquhar, J., Day, J.M., Hauri, E.H., 2013. Anomalous sulphur isotopes in plume lavas reveal deep mantle storage of Archaean crust. Nature 496, 490-494.

Kavecsanszki, D., Moore K., Wall F., 2014. Evolution of silico-carbonatite parental magmas to form the Phalaborwa igneous complex: a complex history of

melting of multiple mantle sources, magma mingling, differentiation and magmatic exsolution, General Meeting of International Mineralogical Association Geological Society of South Africa, Johannesburg, p. 196.

Delavault, H., Chauvel, C., Thomassot, E., Devey, C.W., Dazas, B., 2016. Sulfur and lead isotopic evidence of relic Archean sediments in the Pitcairn mantle plume. Proc. Natl. Acad. Sci. USA. 113, 12952-12956.

Dottin III, J.W., Farquhar, J., Labidi, J., 2018. Multiple sulfur isotopic composition of main group pallasites support genetic links to IIIAB iron meteorites. Geochim. Cosmochim. Acta 224, 276-281.

Eriksson, S., 1989. Phalaborwa: a saga of magmatism, metasomatism and miscibility, Carbonatites: Genesis and evolution. Unwin Hyman London, pp. 221-254.

Farquhar, J., Peters, M., Johnston, D.T., Strauss, H., Masterson, A., Wiechert, U., Kaufman, A.J., 2007. Isotopic evidence for Mesoarchaean anoxia and changing atmospheric sulphur chemistry. Nature, 449, 706-710.

Farquhar, J., Johnston, D.T., Wing, B.A., Habicht, K.S., Canfield, D.E., Airieau, S., Thiemens, M.H., 2003. Multiple sulphur isotopic interpretations of biosynthetic pathways: implications for biological signatures in the sulphur isotope record. Geobiology 1, 27-36.

Farquhar, J., Bao, H., Thiemens, M., 2000. Atmospheric influence of Earth's earliest sulfur cycle. Science 289, 756-758.

Fischer, T., Burnard, P., Marty, B., Hilton, D., Füri, E., Palhol, F., Sharp, Z., Mangasini, F., 2009. Upper-mantle volatile chemistry at Oldoinyo Lengai volcano and the origin of carbonatites. Nature 459, 77-80.

Giuliani, A., Fiorentini, M.L., Martin, L.A., Farquhar, J., Phillips, D., Griffin, W.L., LaFlamme, C., 2016. Sulfur isotope composition of metasomatised mantle

xenoliths from the Bultfontein kimberlite (Kimberley, South Africa): Contribution from subducted sediments and the effect of sulfide alteration on S isotope systematics. Earth Planet. Sci. Lett. 445, 114-124.

Guo, Q., Strauss, H., Kaufman, A.J., Schröder, S., Gutzmer, J., Wing, B., Baker, M.A., Bekker, A., Jin, Q., Kim, S.-T., 2009. Reconstructing Earth's surface oxidation across the Archean-Proterozoic transition. Geology 37, 399-402.

Hofmann, A.W., 1997. Mantle geochemistry: the message from oceanic volcanism. Nature 385, 219-229.

Horstmann, U.E., Verwoerd, W.J., 1997. Carbon and oxygen isotope variations in southern African carbonatites. J.Afric. Earth Sci. 25, 115-136.

Huberty, J.M., Kita, N.T., Kozdon, R., Heck, P.R., Fournelle, J.H., Spicuzza, M.J., Xu, H., Valley, J.W., 2010. Crystal orientation effects in $\delta^{18}O$ for magnetite and hematite by SIMS. Chem. Geol., 276, 269-283.

Kalfoun, F., Ionov, D., Merlet, C., 2002. HFSE residence and Nb/Ta ratios in metasomatised, rutile-bearing mantle peridotites. Earth Planet. Sci. Lett. 199, 49-65.

Kamber, B.S., Collerson, K.D., 1999. Origin of ocean island basalts: a new model based on lead and helium isotope systematics. J. Geophysical Res. Solid Earth 104, 25479-25491.

Kramers, J.D., Mouri, H., 2011. The geochronology of the Limpopo Complex: a controversy solved. Geol. Soc. Am. Mem. 207, 85-106.

Kramers, J.D., Tolstikhin, I.N., 1997. Two terrestrial lead isotope paradoxes, forward transport modelling, core formation and the history of the continental crust. Chem. Geol. 139, 75-110.

Krasnova, N., Petrov, T., Balaganskaya, E., Garcia, D., Moutte, J., Zaitsev, A., Wall, F., 2004. Introduction to phoscorites: occurrence, composition, nomenclature

and petrogenesis, Phoscorites and carbonatites from mantle to mine: the Key example of the Kola Alkaline Province. Mineral. Soc. London, pp. 45-74.

Labidi, J., Cartigny, P. and Moreira, M., 2013. Non-chondritic sulphur isotope composition of the terrestrial mantle. Nature, 501, 208-211.

Labidi, J., Cartigny, P., 2016. Negligible sulfur isotope fractionation during partial melting: Evidence from Garrett transform fault basalts, implications for the late-veneer and the hadean matte. Earth Planet. Sci. Lett. 451, 196-207.

Labidi, J., Cartigny, P., Jackson, M. G., 2015. Multiple sulfur isotope composition of oxidized Samoan melts and the implications of a sulfur isotope 'mantle array'in chemical geodynamics. Earth Planet. Sci. Lett. 417, 28-39.

Lee, W.-J., Wyllie, P.J., 1998. Processes of crustal carbonatite formation by liquid immiscibility and differentiation, elucidated by model systems. J. Petrol. 39, 2005-2013.

Lombaard, A., Ward-Able, N., Bruce, R., 1964. The exploration and main geological features of the copper deposit in carbonatite at Loolekop, Palabora complex. The geology of some ore deposits in Southern Africa 2, 315-337.

Ludwig, K., 2008. User's manual for Isoplot 3.70. Berkeley Geochronology Center Special Publication 4, p. 76.

Lyubetskaya, T., Korenaga, J., 2007. Chemical composition of Earth's primitive mantle and its variance: 1. Method and results. J. Geophysical Research: Solid Earth 112, 1-21.

Magalhães, N., Penniston-Dorland, S., Farquhar, J., Mathez, E.A., 2018. Variable sulfur isotope composition of sulfides provide evidence for multiple sources of contamination in the Rustenburg Layered Suite, Bushveld Complex. Earth Planet. Sci. Lett. 492, 163-173.

Magalhães, N., Farquhar, J., Bybee, G., Penniston-Dorland, S., Rumble, D.; Kinnaird, J.; McCreesh, M., 2019. Multiple sulfur isotopes reveal a possible non-crustal source of sulfur for the Bushveld Province, southern Africa. Geology, https://doi.org/10.1130/G46282.1

Mathez, E., Waight, T.E., 2003. Lead isotopic disequilibrium between sulfide and plagioclase in the Bushveld Complex and the chemical evolution of large layered intrusions. Geochim. Cosmochim. Acta 67, 1875-1888.

Milani, L., Bolhar, R., Cawthorn, R.G., Frei, D., 2017a. In situ LA-ICP-MS and EPMA trace element characterization of Fe-Ti oxides from the phoscorite-carbonatite association at Phalaborwa, South Africa. Miner. Depos. 52, 747-768.

Milani, L., Bolhar, R., Frei, D., Harlov, D.E., Samuel, V.O., 2017b. Light rare earth element systematics as a tool for investigating the petrogenesis of phoscorite-carbonatite associations, as exemplified by the Phalaborwa Complex, South Africa. Miner. Depos. 52, 1105-1125.

Mitchell, R.H., Krouse, H.R., 1975. Sulphur isotope geochemistry of carbonatites. Geochim. Cosmochim. Acta 39, 1505-1513.

Penniston-Dorland, S.C., Mathez, E.A., Wing, B.A., Farquhar, J., Kinnaird, J.A., 2012. Multiple sulfur isotope evidence for surface-derived sulfur in the Bushveld Complex. Earth Planet. Sci. Lett. 337, 236-242.

Richardson, S., Shirey, S., Harris, J., Carlson, R., 2001. Archean subduction recorded by Re–Os isotopes in eclogitic sulfide inclusions in Kimberley diamonds. Earth Planet. Sci. Lett. 191, 257-266.

Richardson, S.H., Shirey, S.B., 2008. Continental mantle signature of Bushveld magmas and coeval diamonds. Nature 453, 910-913.

Rudashevsky, N., Kretser, Y.L., Rudashevsky, V., Sukharzhevskaya, E., 2004. A

review and comparison of PGE, noble-metal and sulphide mineralization in phoscorites and carbonatites from Kovdor and Phalaborwa. Phoscorites and Carbonatites from Mantle to Mine: the Key Example of the Kola Alkaline Province", eds. F. Wall and AN Zaitev, The Mineralogical Society of Great Britain and Ireland, London, 375-405.

Rudnick, R.L., 1995. Making continental crust. Nature 378, 571-578.

Sasada, T., Hiyagon, H., Bell, K., Ebihara, M., 1997. Mantle-derived noble gases in carbonatites. Geochim. Cosmochim. Acta 61, 4219-4228.

Scoates, J.S., Wall, C.J., 2015. Geochronology of layered intrusions, Layered intrusions. Springer, pp. 3-74.

Shimizu, N. and Hart, S.R., 1982. Isotope fractionation in secondary ion mass spectrometry. J. App. Physics 53, 1303-1311.

Thomassot, E., Cartigny, P., Harris, J., Lorand, J., Rollion-Bard, C., Chaussidon, M., 2009. Metasomatic diamond growth: A multi-isotope study ($^{13}C$, $^{15}N$, $^{33}S$, $^{34}S$) of sulphide inclusions and their host diamonds from Jwaneng (Botswana). Earth Planet. Sci. Lett. 282, 79-90.

Veksler, I., Nielsen, T., Sokolov, S., 1998. Mineralogy of crystallized melt inclusions from Gardiner and Kovdor ultramafic alkaline complexes: implications for carbonatite genesis. J. Pet. 39, 2015-2031.

Verwoerd, W., Du Toit, M., 2006. The Phalaborwa and Schiel complexes. The Geology of South Africa 291, p. 299.

Vielreicher, N.M., Groves, D.I., Vielreicher, R.M., 2000. The Phalaborwa (Palabora) deposit and its potential connection to iron-oxide copper-gold deposits of Olympic Dam Type. Hydrothermal Iron-Oxide Copper-Gold and Related Deposits. A Global Perspective", ed. TM Porter, PGC Publishing, Adelaide, Australia 1, 321-329.

Whitehouse, M.J., 2013. Multiple sulfur isotope determination by SIMS: Evaluation of reference sulfides for Δ33S with observations and a case study on the determination of $\Delta^{36}S$. Geostand. Geoanal. Res. 37, 19-33.

Wilson, A.H., 2012. A chill sequence to the Bushveld Complex: insight into the first stage of emplacement and implications for the parental magmas. J. Pet. 53, 1123-1168.

Wu, F.-Y., Yang, Y.-H., Li, Q.-L., Mitchell, R.H., Dawson, J.B., Brandl, G., Yuhara, M., 2011. In situ determination of U–Pb ages and Sr–Nd–Hf isotopic constraints on the petrogenesis of the Phalaborwa carbonatite Complex, South Africa. Lithos 127, 309-322.

Zeh, A., Ovtcharova, M., Wilson, A. H., & Schaltegger, U., 2015. The Bushveld Complex was emplaced and cooled in less than one million years–results of zirconology, and geotectonic implications. Earth Planet. Sci. Lett. 418, 103-114.

Zirakparvar, N.A., Mathez, E.A., Scoates, J.S., Wall, C.J., 2014. Zircon Hf isotope evidence for an enriched mantle source for the Bushveld Igneous Complex. Contrib. Mineral. Petrol. 168, 1050-1068.

**Figure captions**

**Figure 1**

(a) Map of southern Africa showing the major tectonic domains and the location of the Phalaborwa Complex. (b) Simplified geological map of the main lithologies and the Loolekop pipe (shown in more detail in (c)). (d) Simplified geological cross-section through the Loolekop pipe. Abbreviations: DB = Damara Belt, NNP =

Namaqua-Natal Province, RP = Rehoboth Province. Modified after Verwoerd and du Toit (2006) and Wu et al. (2011).

**Figure 2**

(A) Phoscorite B66: Discrete pyrite (pale cream) intergrown with Cu-sulphides; chalcopyrite (yellow) is largely exsolved in bornite (brown). (B) Phoscorite B66: Chalcopyrite exsolutions (yellow) appear as spindle-shaped laths that taper at intersections with bornite (purple). (C) Transgressive Carbonatite B61B: Sulphide mineralization with minor pyrite (white) and intergrown chalcopyrite (yellow) - bornite (purple). Magnetite (gray) is also developed along the bornite margins. (D) Transgressive Carbonatite B61B: Vein with bornite (purple) partially intergrown with chalcopyrite (yellow). Late-stage chalcocite (light blue), valleriite (brown), and magnetite (gray) are also present. (E) Banded Carbonatite GC813A: Anhedral bornite (pink, orange) and minor chalcopyrite (yellow). Bornite contains partially exsolved chalcopyrite laths (centre, top right), whereas most of the exsolution lamellae are chalcocite (bluish) following {100}. (F) Banded Carbonatite GC813A: Bornite (brown) mineralization interstitial in magnetite with limited chalcopyrite exsolution (yellow) and major chalcocite (light blue) developing a myrmekite-type pattern. (G) Phoscorite B66: Discrete bornite crystal (brown, centre top) with chalcopyrite exsolutions (yellow) representing an early sulphide event. Chalcocite in veinlets (light blue, centre) and abundant valleriite as rim around sulphides and gangue minerals formed during the latest phase of copper mineralization. (H) Phoscorite B66: Late-stage chalcocite veinlets (light blue) follow cracks in ilmenite (pinkish-gray) and magnetite (gray) or rim apatite crystals (dark). Abbreviations: Ap = apatite; Brn = bornite, Cal = calcite, Cc = chalcocite, Cpy = chalcopyrite, Ilm = ilmenite, Mt =

magnetite, Pyr = pyrite,Vall = valleriite.

**Figure 3**

Microphotographs of phoscorite B66 (as in Fig. 2G); (A) spot targets (green rectangles: Pb analysis, blue rectangles: S isotope analysis) for SIMS analysis with the white rectangle corresponding to the area shown in B, and (B) spots after SIMS analysis. Note that SIMS spots are restricted to chalcocite and do not represent mixing of different sulphide species.

**Figure 4**

Multi-trace-element diagram (normalized to PRIMA: Lyubetskaya and Korenaga, 2007), showing representative average whole-rock compositions of phoscorite, banded carbonatite, and transgressive carbonatite from the PC. Note remarkable similarity in composition: strongly depleted Cs, Rb, Ba, and Pb; slightly depleted Sr and Eu; distinctly negative anomalies for Nb, Ta, Zr, and Hf. Nb/U and Ce/Pb ratios are different from the values for the MORB and OIB mantle (Hofmann 1997), and coupled with positive Pb anomalies, rule out significant crustal contribution after extraction of asthenospheric and or lithospheric mantle melts. Ratios of Nb/Ta and Zr/Hf deviate from chondritic values, indicating non-CHARAC (ionic charge and radius controlled) behavior (Bau, 1996), consistent with the SCLM metasomatism.

**Figure 5**

Diagrams of $^{207}Pb/^{206}Pb$ vs. $^{204}Pb/^{206}Pb$ (A) and $^{207}Pb/^{204}Pb$ vs. $^{206}Pb/^{204}Pb$ (B) showing isotope data for individual sulphides from phoscorites, and banded and transgressive carbonatites (error ellipses and regression line in A were constructed

using ISOPLOT 3.7 (Ludwig, 2008)). Evolution curves for terrestrial reservoirs are from Kramers and Tolstikhin (1997) and Kamber and Collerson (1999), Pb isotope data for the BC sulphides are from Mathez and Waight (2002). An estimate of the average Pb isotopic composition of Archaean lower continental crust is also shown for comparison (Bolhar et al., 2007).

**Figure 6**

Multiple sulfur and lead isotope compositions of sulphides and host rocks (phoscorite and carbonatites). (A) $\delta^{33}S$ vs. $\delta^{34}S$ values measured by SIMS; mantle range used to represent uncontaminated mantle is from Labidi et al. (2013). (B) $\delta^{33}S$ vs. $\delta^{34}S$ values for sulphide mineral separates and sulphur extracts from bulk rocks. Grey areas in A and B define isotope data produced by mass-dependent fractionation processes (cf. Bekker et al., 2004); slopes are from Farquhar et al. (2003). (C) $\Delta^{33}S$ vs. $\delta^{34}S$ values for sulphides measured by SIMS (see A for figure legend); fields for the Transvaal Supergroup sediments (Guo et al., 2009), Rustenberg Layered Suite of the BC (Penniston-Dorland et al., 2012; Magalhães et al., 2018), and uncontaminated mantle ($\Delta^{33}S$ = 0.006 ± 0.008 ‰: Labidi and Cartigny, 2016) are also shown. (D) $\Delta^{33}S$ vs. $\delta^{34}S$ values for sulphide mineral separates and sulphur extracts from bulk rocks (see B for figure legend). Note that the range of $\Delta^{33}S$ values for the PC is larger than that for the BC. (E) $\Delta^{36}S$ vs. $\Delta^{33}S$ values for sulphur extracts from bulk rocks measured with the DI-IRMS method; two thick dashed lines represent the array found in Archaean sediments ($\Delta^{36}S/\Delta^{33}S$ = -0.9 to -1.5). The thick dotted line represents mass-dependent S isotope fractionation ($\Delta^{36}S/\Delta^{33}S$ = -7), and was adopted from Farquhar et al. (2007). (F) $\Delta^{33}S$ vs. $\Delta^{207}Pb/^{204}Pb$ (calculated as a percentage difference between the isochron and measured $^{207}Pb/^{204}Pb$ values for any given $^{206}Pb/^{204}Pb$ ratio).

**Figure 7**

Histograms of SIMS $\Delta^{33}S$ data grouped by the type of host rock and sulphide minerals. Note that $\Delta^{33}S$ values overlap for phoscorite and banded carbonatite, whereas transgressive carbonatite spans the entire range. Valleriite shows the most extreme $\Delta^{33}S$ values (> 1 ‰).

**Figure 8**

Cartoon illustrating the events giving rise to MIF-S and crustal Pb in sulphides within the PC. (A) Prior to ca. 2.43 Ga sulphur from volcanic eruptions underwent photochemical reactions in an oxygen-poor atmosphere, resulting in MIF. Sulphur and Pb with a continental crust signature were deposited with marine sediments, followed by subduction, and were transferred via slab dehydration into an overlying mantle wedge, forming metasomatized SCLM. (B) Magmatism commenced with impingement of the rising mantle plume onto the base of the SCLM; initially partial melting affected mostly fertile portions within the SCLM; melts derived from the asthenospheric and lithospheric mantle mixed and led to the PC magmatism. (C) Plume head spread and magmatism continued, affecting less fertile portions of the SCLM and mobilizing MIF-S and crustal Pb, which were then incorporated into the PC sulphides at ca. 2.06 Ga. Cartoons are not to scale.

Figure 1

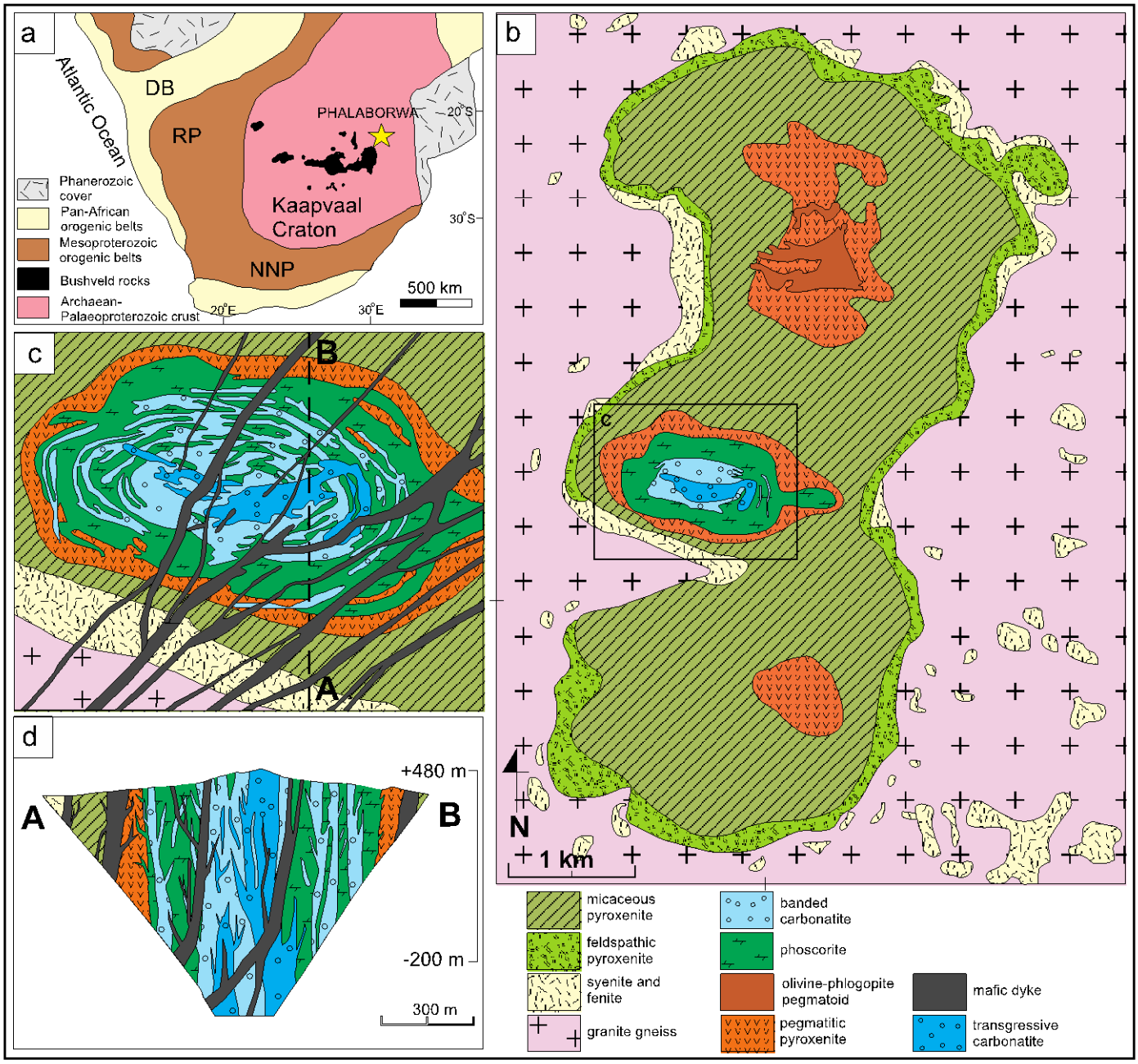
a
Atlantic Ocean
DB
RP
PHALABORWA
20°S
Kaapvaal
Craton
30°S
NNP
500 km
20°E
30°E
Phanerozoic cover
Pan-African orogenic belts
Mesoproterozoic orogenic belts
Bushveld rocks
Archaean-Palaeoproterozoic crust
b
c
B
A
d
+480 m
A
B
-200 m
300 m
N
1 km
micaceous pyroxenite
feldspathic pyroxenite
syenite and fenite
granite gneiss
banded carbonatite
phoscorite
olivine-phlogopite pegmatoid
pegmatitic pyroxenite
mafic dyke
transgressive carbonatite

Figure 2

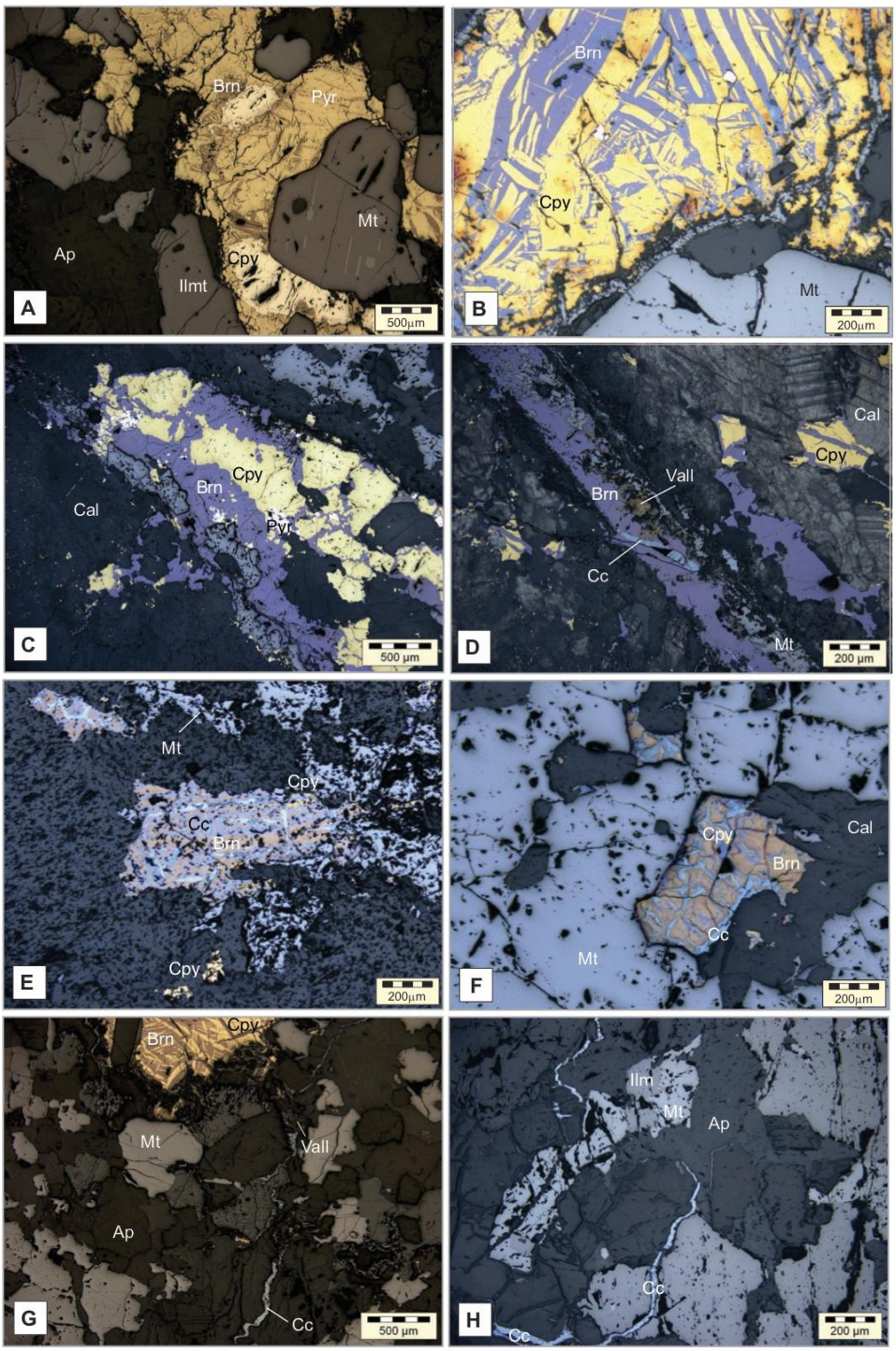
A
Brn
Pyr
Mt
Ap
Cpy
Ilmt
500µm
B
Brn
Cpy
Mt
200µm
C
Cpy
Brn
Cal
Pyr
500 µm
D
Cal
Cpy
Vall
Brn
Cc
Mt
200 µm
E
Mt
Cpy
Cc
Brn
Cpy
200µm
F
Cpy
Cal
Brn
Cc
Mt
200µm
G
Brn
Cpy
Mt
Vall
Ap
Cc
500 µm
H
Ilm
Mt
Ap
Cc
Cc
200 µm

Figure 3

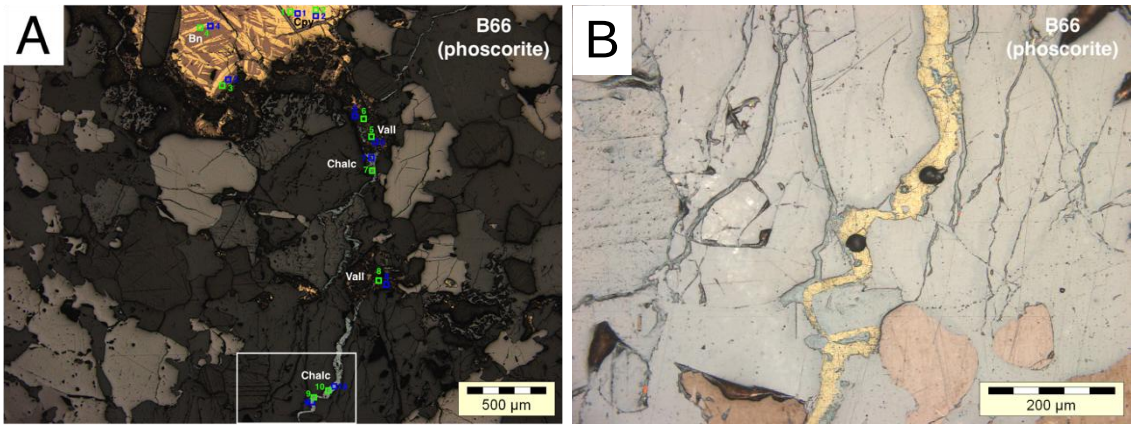
A
B66
(phoscorite)
Bn
Cpy
Vall
Chalc
Vall
Chalc
500 µm
B
B66
(phoscorite)
200 µm

Figure 4

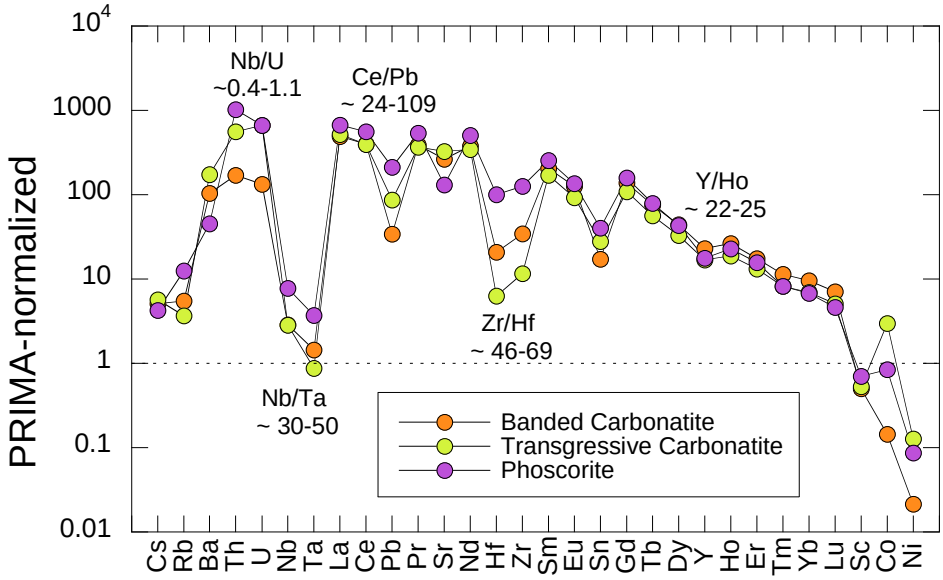
PRIMA-normalized
10^4
1000
100
10
1
0.1
0.01
Nb/U
~0.4-1.1
Ce/Pb
~ 24-109
Y/Ho
~ 22-25
Zr/Hf
~ 46-69
Nb/Ta
~ 30-50
Banded Carbonatite
Transgressive Carbonatite
Phoscorite
Cs Rb Ba Th U Nb Ta La Ce Pb Pr Sr Nd Hf Zr Sm Eu Sn Gd Tb Dy Y Ho Er Tm Yb Lu Sc Co Ni

Figure 5

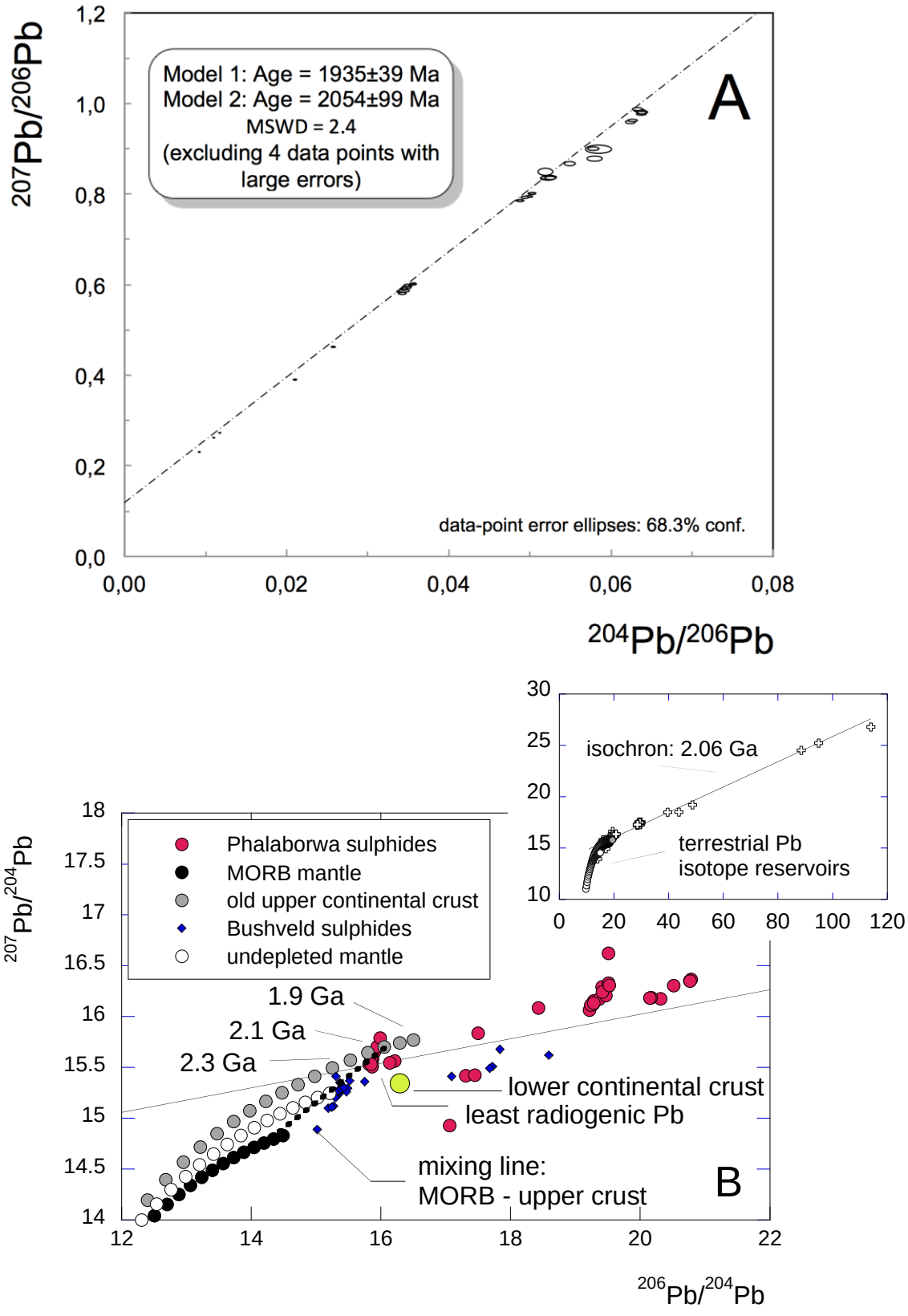
Model 1: Age = 1935±39 Ma
Model 2: Age = 2054±99 Ma
MSWD = 2.4
(excluding 4 data points with large errors)
A
data-point error ellipses: 68.3% conf.
207Pb/206Pb
204Pb/206Pb
1,2
1,0
0,8
0,6
0,4
0,2
0,0
0,00
0,02
0,04
0,06
0,08
isochron: 2.06 Ga
terrestrial Pb isotope reservoirs
30
25
20
15
10
0
20
40
60
80
100
120
Phalaborwa sulphides
MORB mantle
old upper continental crust
Bushveld sulphides
undepleted mantle
1.9 Ga
2.1 Ga
2.3 Ga
lower continental crust
least radiogenic Pb
mixing line:
MORB - upper crust
B
207Pb/204Pb
206Pb/204Pb
18
17.5
17
16.5
16
15.5
15
14.5
14
12
14
16
18
20
22

Figure 6

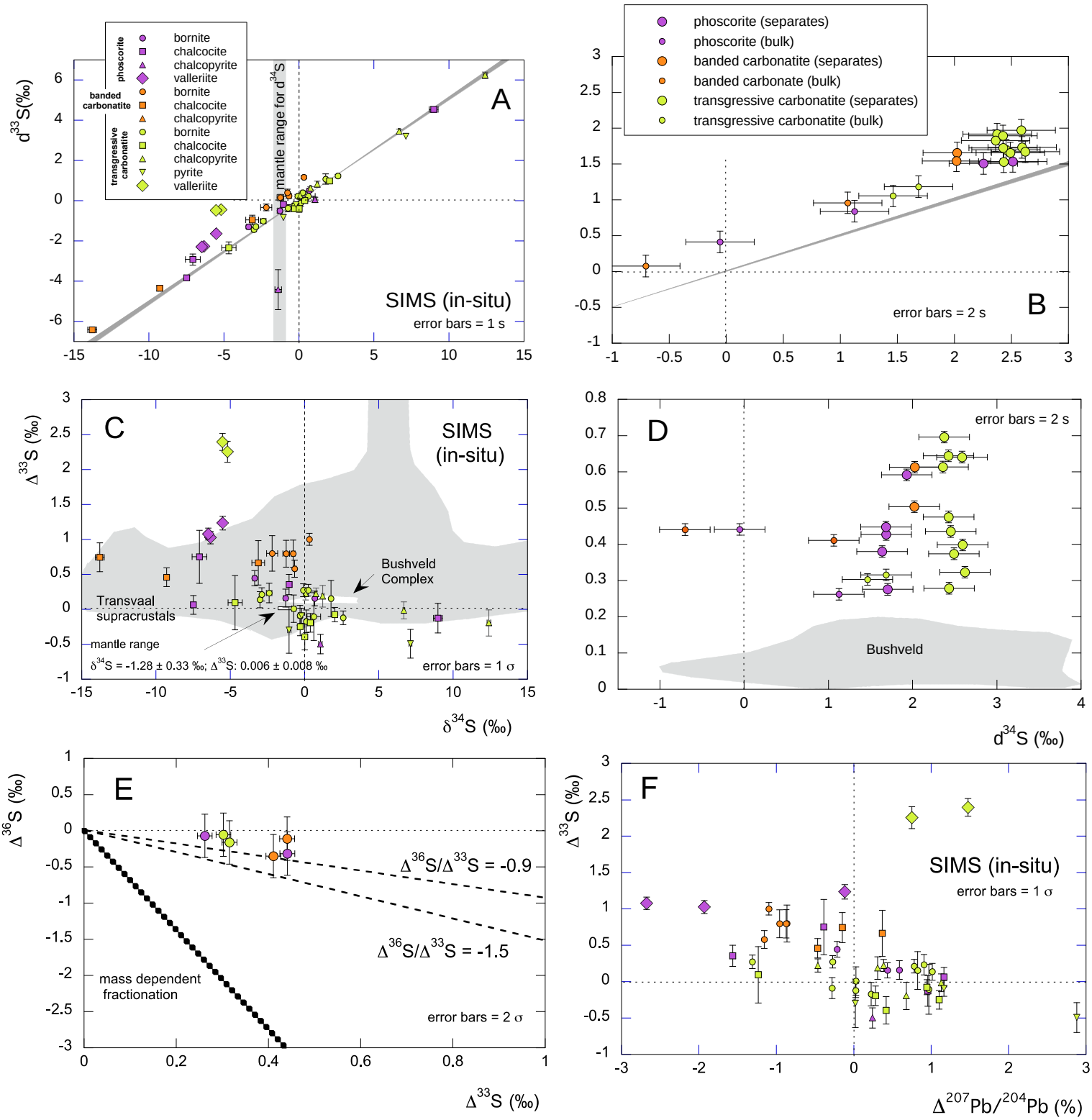
A
phoscorite
banded carbonatite
transgressive carbonatite
bornite
chalcocite
chalcopyrite
valleriite
bornite
chalcocite
chalcopyrite
bornite
chalcocite
chalcopyrite
pyrite
valleriite
mantle range for d34S
SIMS (in-situ)
error bars = 1 s
d33S(‰)
B
phoscorite (separates)
phoscorite (bulk)
banded carbonatite (separates)
banded carbonate (bulk)
transgressive carbonatite (separates)
transgressive carbonatite (bulk)
error bars = 2 s
C
SIMS (in-situ)
Bushveld Complex
Transvaal supracrustals
mantle range
δ34S = -1.28 ± 0.33 ‰; Δ33S: 0.006 ± 0.008 ‰
error bars = 1 σ
Δ33S (‰)
δ34S (‰)
D
error bars = 2 s
Bushveld
d34S (‰)
E
Δ36S/Δ33S = -0.9
Δ36S/Δ33S = -1.5
mass dependent fractionation
error bars = 2 σ
Δ36S (‰)
Δ33S (‰)
F
SIMS (in-situ)
error bars = 1 σ
Δ33S (‰)
Δ207Pb/204Pb (‰)

Figure 7

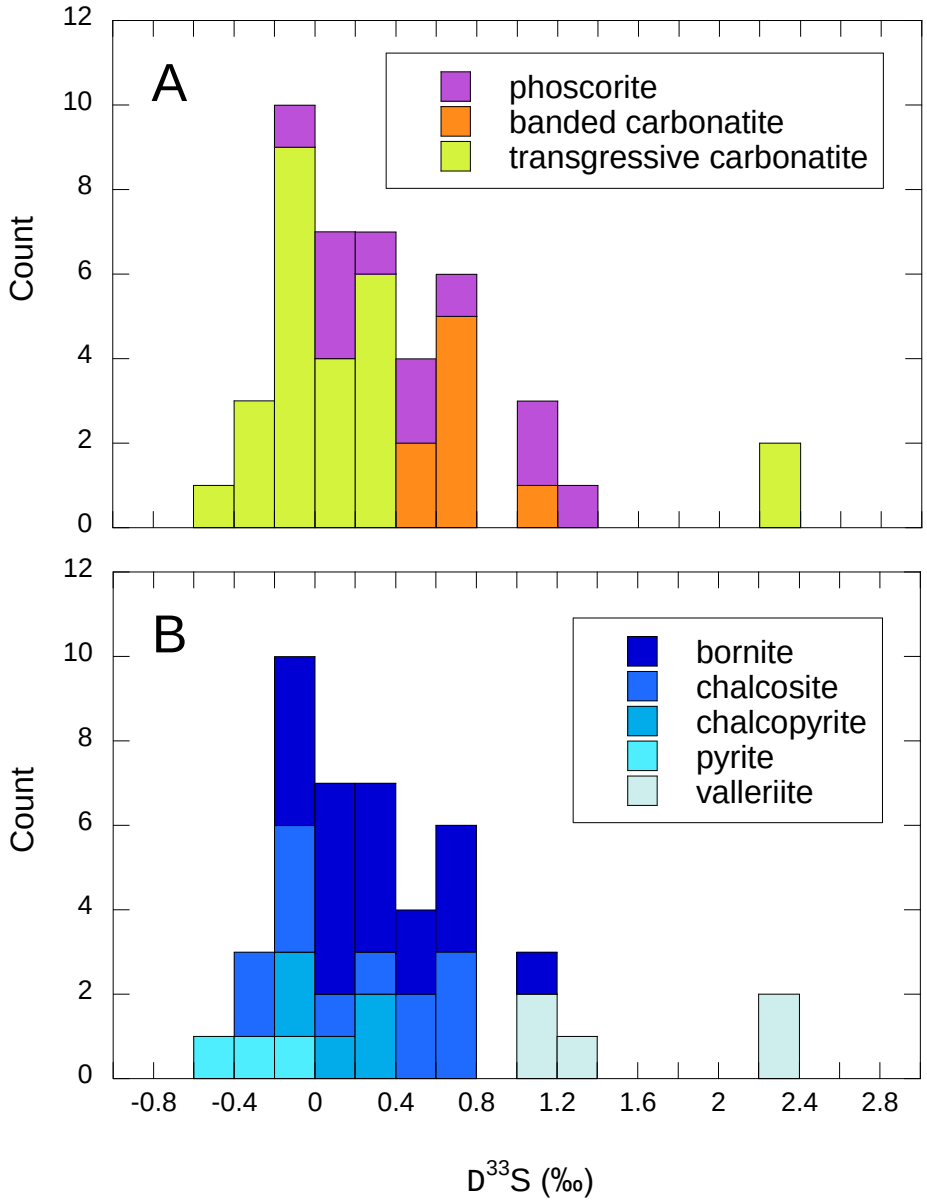
A
phoscorite
banded carbonatite
transgressive carbonatite
Count
B
bornite
chalcosite
chalcopyrite
pyrite
valleriite
Count
0
2
4
6
8
10
12
-0.8
-0.4
0
0.4
0.8
1.2
1.6
2
2.4
2.8
D33S (‰)

Figure 8

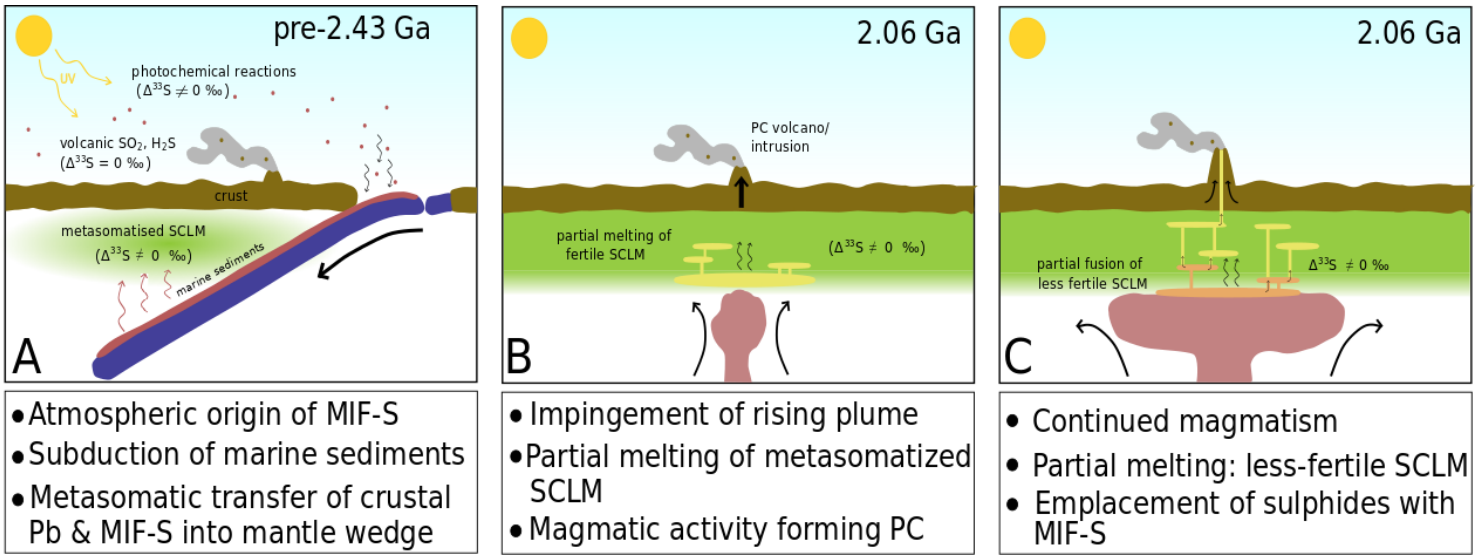


- Atmospheric origin of MIF-S
- Subduction of marine sediments
- Metasomatic transfer of crustal Pb & MIF-S into mantle wedge

- Impingement of rising plume
- Partial melting of metasomatized SCLM
- Magmatic activity forming PC

- Continued magmatism
- Partial melting: less-fertile SCLM
- Emplacement of sulphides with MIF-S

**Table 1: Stages of Sulphide Mineralization at Phalaborwa**

| stages | lithologies | dominant minerals | textures | microphotograph in Figure 2 |
|---|---|---|---|---|
| stage 1 (earliest) | phos, carb | bn, chalc | disseminated to interstitial, droplets, parallel to magnetite banding; exsolution cpy-bn | Phos B66: A |
| stage 2 (main) | carb | bn, cpy (±pyr, cub) | fracture-filling, irregular to aligned, exsolution from bn to cpy, then chalc; myrmecitic texture in bn | TC B61B: D; BC GC813A: E & F |
| stage 3 (low T) | phos | chalc, vall | stockwork of cross-cutting veins, also as rims | Phos B66: G & H |

phos=phoscorite, carb=carbonatite, bn=bornite, chalc=chalcosite, cpy=chalcopyrite, cub=cubanite, vall=valleriite; T = temperature